

Cassini Program

Titan Atmospheric Modeling Working Group Final Report

D-105424

Revision 0

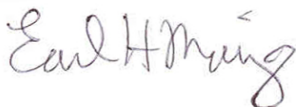
Prepared By:



Scott G. Edgington
Cassini Deputy Project Scientist

3/24/20__
Date

Approved By:



Earl Maize
Cassini Project Manager

3/24/20__
Date

March 2020



Jet Propulsion Laboratory
California Institute of Technology
4800 Oak Grove Drive
Pasadena, CA 91109-8099

Change Log

Revision	Date	Changed By	Section(s)	Description
0	March 2020	S.G. Edgington		Document created

Table of Contents

1.	Title, Affiliations, and Acknowledgements	4
2.	Preface	5
3.	Timeline of Key Events	6
4.	TAMWG Report	7
5.	References	
6.	Appendices:	
	1. Safe Flyby Altitude for T7	32
	2. Update on the Discrepancy in Mass Density Inferred by AACS and INMS	33

Titan Atmospheric Modeling Working Group Final Report

Roger V. Yelle¹, Darrell F. Strobel¹, Ralph Lorenz³, Tom Burk⁴, Dylan Boone⁴, Earl H. Maize⁴,
Scott G. Edgington^{4,5}, Linda J. Spilker⁴, Trina L. Ray⁴

¹Lunar and Planetary Laboratory, University of Arizona, Tucson, AZ

²The Johns Hopkins University, Baltimore, MD

³Applied Physics Laboratory, The Johns Hopkins University Columbia, MD.

⁴Jet Propulsion Laboratory, California Institute of Technology, Pasadena, CA

⁵Corresponding Author: scott.g.edgington@jpl.nasa.gov

Acknowledgement: The research was carried out at the Jet Propulsion Laboratory, California Institute of Technology, under a contract with the National Aeronautics and Space Administration. © 2020. All rights reserved.

Preface

by **Scott G. Edgington**

The importance of understanding Titan's upper atmosphere, through which the Huygens probe descended and the Cassini orbiter flew many times during its mission, cannot be understated. The Titan Atmospheric Modeling Working Group (TAMWG) was formed by Cassini-Huygens Project Scientist and Project Manager with this goal in mind.

The key objectives of TAMWG were to provide the best scientific assessment of the density profile of Titan's atmosphere and its associated uncertainties to the Cassini-Huygens Project Management to ensure that both spacecraft could safely execute their missions. Early on, the support of the Huygens probe mission was the key objective. After successfully landing the first human made object on the surface of Titan, the focus of TAMWG became Cassini's flybys through Titan's upper atmosphere. A combination of science and engineering data was used as each team/instrument strove to provide better and better insight into this tricky problem.

Key contributions were made by Titan atmospheric scientists representing the Huygens Probe instruments teams (e.g. Huygens Atmospheric Structure Instrument) and Cassini's instrument teams (e.g. the Ultraviolet Imaging Spectrometer and the Ion and Neutral Mass Spectrometer) and by engineers from Cassini's Navigation team and Attitude and Articulation Control System team. Dr. Roger Yelle, Dr. Darrell Strobel, and Cassini's Mission Planning Team coordinated these efforts.

Because of the surprises and changes to Titan's atmosphere as the mission progressed, as well as the subtle calibration of instruments, TAMWG was active throughout most of the 13 years of the Cassini mission. The work of TAMWG continued until the very end of Cassini's mission because newly collected science and engineering data were key to providing information about the atmospheric conditions encountered during all close Titan flybys. Reports were made periodically to the Titan Working Group, the Project Science Group, and Mission Planning.

This final report reflects the efforts of the TAMWG.

Best Regards,

Scott G. Edgington, Ph.D.

Cassini Deputy Project Scientist/Saturn Target Working Team Lead/CIRS Investigation Scientist
Jet Propulsion Laboratory, California Institute of Technology

Timeline of key developments

- October 15, 1997: Cassini-Huygens Launches
- June 30, 2004: Saturn Orbit Insertion
- October 26, 2004: First Titan flyby, key data for Huygens release (TA – 1174 km)
- January 14, 2005: Huygens Probe descends into Titan's Atmosphere
- April 16, 2005: First "Close" Titan Flyby (T5 - 1027 km)
- July 22, 2006: Key northern hemisphere close flyby (T16 - 950 km)
- June 21, 2010: Closest Titan Flyby (T70 - 878km)
- April 22, 2017: Final Titan Flyby
- September 15, 2017: End of Cassini's mission

—

Investigations of Titan's Atmosphere by the Titan Atmosphere Working Group (TAMWG)

Roger V. Yelle¹, Darrell F. Strobel¹, Ralph Lorenz³, Tom Burk⁴, Dylan Boone⁴, Scott G. Edgington^{4,5}, Linda J. Spilker⁴, Trina L. Ray⁴, Earl H. Maize⁴, and the Titan Atmospheric Modeling Working Group

¹Lunar and Planetary Laboratory, University of Arizona, Tucson, AZ

²The Johns Hopkins University, Baltimore, MD

³Applied Physics Laboratory, The Johns Hopkins University Columbia, MD.

⁴Jet Propulsion Laboratory, California Institute of Technology, Pasadena, CA

⁵Corresponding Author: scott.g.edgington@jpl.nasa.gov

19 July 2018 (revised 21 March 2020)

Introduction

The Titan Atmosphere Working Group (TAMWG) served as the interface between the Cassini science team and the spacecraft, engineering and operations teams. TAMWG played several different roles in the course of the mission. In the mission development phase, TAMWG was dedicated to producing the best prediction for the density structure and composition of Titan's atmosphere along with the uncertainties in these properties. These models were used in designing the orbiter and probe missions. During the orbiter mission and its extensions, TAMWG was instrumental in planning Titan flybys, especially in modeling the minimum flyby altitudes. Finally, TAMWG helped organize the intercomparisons between various density measurements made throughout the mission, by both the science teams and the spacecraft teams.

The group did not have a fixed membership. Cassini and Huygens scientists participated according to their interests and as their expertise was required. TAMWG was chaired by Roger Yelle from its inception. Titan Interdisciplinary Scientist, Darrell Strobel, participated throughout its existence. The group included representatives from Mission Planning, Attitude and Articulation Control Subsystem (AACCS), and Navigation (NAV) teams. Participation from the Composite Infrared Spectrometer (CIRS) and Visual and Infrared Spectrometer (VIMS) teams was important in the mission development phase, when the focus was on the entire atmosphere of Titan. The Ion and Neutral Mass Spectrometer (INMS) and Ultraviolet Imaging Spectrograph Subsystem (UVIS) representatives participated in this phase also, as well as in TAMWG activities during the orbiter phase, when emphasis was on the upper atmosphere and in the intercalibration of density measurements.

In this document, we briefly review some of the challenges and accomplishments of TAMWG and provide a summary of its operating procedures.

With the completion of the Cassini mission, we have an opportunity to review of knowledge of Titan's atmosphere. For the upper atmosphere, a main result is the extreme variability of the upper atmospheric densities and temperature. This has, so far, precluded development of comprehensive empirical models for the atmosphere in terms of the usual geophysical variables (latitude, longitude, local time, solar activity, etc.). However, the large suite of measurements implies that the variability is well characterized and the mean state well determined. Future work on Cassini Titan data may produce these models for Titan's upper atmosphere.

Pre-Encounter Activities

The Cassini-Huygens project supported the development of Titan atmospheric models to aid in the planning of the Huygens probe and Cassini orbiter missions. These results are summarized in Yelle et al. (1997). The Huygens probe mission required models for the full atmosphere, from the surface to the exobase. The Cassini orbital mission was concerned with densities in the upper atmosphere, which were to be sensed directly, but the altitude of the upper atmosphere depends on conditions in the lower atmosphere, which are therefore also important. Prior to the Cassini-Huygens Mission, the only measurements of densities in the upper atmosphere were those from the Voyager mission in the early 1980's (Smith et al., 1982). Observations in the mid-infrared by the Voyager Infrared Interferometer, Radiometer, and Spectrometer Subsystem (IRIS) instrument constrained the structure of the stratosphere. Radio occultation data (ingress and egress) obtained by the Radio Science Subsystem (RSS) constrained the profile in the troposphere and lower stratosphere, and mid-infrared observations by IRIS helped anchor this profile (Lindal et al., 1983). All of this information was used by Yelle et al. (1997) in the construction of a range of atmospheric models. There were significant uncertainties in the models related to the composition of the atmosphere, which was not uniquely constrained by Voyager measurements. In particular, the argon abundance was constrained to between 0 and 10% (Strobel et al., 1993), while observational data could be fit by methane mole fractions from 1 to 5% (Courtin et al., 1995; Yelle et al., 1997). The recommended model used in the Cassini-Huygens planning had an upper atmospheric temperature of 175 K, an argon mole fraction of 2%, and a methane mole fraction (in the stratosphere) of 3%. These can be compared to the measured argon mole fraction of 3×10^{-5} and methane mole fraction of 1.5% from the Huygens probe (Niemann et al., 2010) and a mean upper atmospheric temperature of 150 K (Snowden et al., 2013).

In addition to the Voyager measurements, Titan's mesosphere was monitored through observations of ground-based stellar occultations (Sicardy et al., 1999, Hubbard et al., 1993). These measurements provided estimates of the atmospheric temperature near 0.1 Pa, the zonal wind speeds in the atmosphere, and the spectrum of waves in the atmosphere. All of these characteristics were important for mission planning, especially for the Huygens probe. The atmospheric temperature profile affected the Huygens descent rate. The zonal winds affected the horizontal drift rate of the probe and its final longitude. The waves also affected the descent rate of the probe and in particular could have triggered an early release of the parachute. The possible effects of gravity waves and wind shear are discussed in Strobel and Sicardy (1997).

The atmospheric models were used for planning the probe mission in a variety of ways. The probe trajectory depended on the structure of the atmosphere, principally the profile of density with altitude. The profile affected the altitude at which descent measurements could begin, as well as the total duration of parachute descent. Of particular importance was the calculation of heat loads on the probe and the ablation of the heat shield. The Ar and CH₄ mole fractions were critical parameters in calculations of the radiative heat load on the probe during entry (e.g. the CH₄ thermochemistry occurring in front of the heat shield produced CN radicals which

radiate in their B_X band and were the major heat load delivered to the heat shield). The atmospheric models were also critical in choosing the entry angle for the probe, to minimize both instantaneous and integrated heating and to ensure that the probe was captured by Titan. All of these studies were conducted by Alcatel, the Huygens probe prime contractor, based in Cannes, France. (Note that company was Aerospatiale when selected to build Huygens in 1990, but in the progressive waves of consolidation of the European aerospace industry became part of Alcatel in 1998, then Alcatel Alenia Space in 2005, and since 2007, is now part of Thales Alenia Space). Because of intellectual property consideration, TAMWG had limited visibility into activities at Alcatel. However, information was provided by TAMWG and results were reported back.

Needless to say, the Huygens probe mission was successful. The measured atmosphere was within the range specified by the pre-encounter models. Nevertheless, these models were updated for the orbital mission, based on newer observations, including remote sensing measurements by instruments on the Cassini orbiter.

Orbital Mission Activities

Just prior to Cassini's arrival at Saturn, a number of significant advances in Titan studies led to development of a new set of atmospheric models. These advances included a reanalysis of the Voyager Ultraviolet Spectrometer (UVS) occultation data (Vervack et al., 2004), extensive analysis of ground-based stellar occultation observations in 2003 (Sicardy et al., 2004), and a fortuitous occultation of the Crab Nebula, a bright X-ray source (Mori et al., 2004). Once in orbit around Saturn, observations were made by the Cassini CIRS and VIMS remote sensing instruments during the first distant Titan encounter (T0). These new data and new analyses led to a revision of the Yelle et al. (1997) models. The new models differed significantly from the 1997 models in terms of composition and upper atmospheric temperature. New information on composition came primarily from Cassini CIRS observations, which determined a best estimate for the CH₄ mole fraction in the stratosphere of 1.8%. This, coupled with Voyager constraints, implied a low abundance of Ar. The revised recommended model adopted the CH₄ mole fraction of 1.8% and an Ar mole fraction of 0%. These values are quite close to the currently accepted values of 1.4% and 30 ppm (cf. Lellouch et al., 2014). The upper atmospheric temperature was also revised from 175 K (from Smith et al., 1982) to 150 K (from Vervack et al., 2004). It was the judgement of TAMWG that the revised analysis in Vervack et al. (2004) was superior to the early analysis by Smith et al. (1982) and, in fact, the mean temperature of Titan's upper atmosphere is close to 150 K. These efforts were described in a report, delivered to the project on 15 October 2004.

The main goal of the Cassini mission planning team and TAMWG was to balance the desire for deep penetration into Titan's atmosphere with spacecraft safety. The situation is well described in the article by D. Seal (Seal and Bittner, 2017). Deeper penetration into the atmosphere would provide precious information on atmospheric composition and temperatures in previously unexplored regions but, if the spacecraft encountered densities that were too large, the torque on the spacecraft would exceed the thruster control authority causing the spacecraft to tumble out of control. Tumbling would likely not result in loss of the spacecraft but would cause the spacecraft to enter safe mode resulting in the loss of scientific observations just after closest approach, as well as an unwelcome disruption of the mission plan. The level at which the torque on the spacecraft would exceed the control authority of the thrusters is called the tumble density. Practically, this occurs when thrusters are firing at a 100% duty cycle (over an interval of time based on s/c momentum inertia and response to torque), i.e. no further increase is possible.

It is therefore convenient to describe each Titan encounter in terms of the maximum thruster duty cycle during the pass (Sarani 2004). Tumble density is not a fixed parameter but was slightly different for each flyby. The spacecraft attitude obviously affects the torque experienced for a fixed density. Additionally, the performance of the thrusters varies, degrading slowly over time until the thrusters are recharged. Results are shown in Table 1. The highest duty cycle reached was 69% on T52. Many passes reached thruster duty cycles greater than 40%.

Due to uncertainties in the density profile, it was decided to approach the atmosphere carefully (e.g. see Appendix 1). The first penetration of the atmosphere during the Titan (TA) flyby occurred at an altitude of 1174 km, TB dipped to 1192 km, T5 to 1027 km, T7 to 1075 km, T16 to 950 km, and finally T70 to 878 km, the lowest altitude Titan flyby of the mission. There were several reasons for this cautious approach. The first measurements at relatively high altitude provided a check on atmospheric models, which could then be refined and extrapolated more accurately to lower altitudes. Additionally, the spacecraft targeting accuracy for the first few flybys had not yet reached the phenomenal levels that became routine in later flybys. Finally, TA functioned as an instrument check out, verifying that instruments built more than 7 years earlier still functioned as expected. In fact, a flaw in the INMS programming was discovered in the analysis of TA data and subsequently corrected in time for TB (Yelle et al., 2006).

TAMWG was exceedingly active during the first years of the Cassini mission, holding roughly bimonthly telecons as well as face-to-face meetings at Project Science Group (PSG) meetings. Each deep pass through the atmosphere (below ~1200 km) was quickly analyzed in detail both by the INMS team and the AACS team. If available, UVIS occultations were also considered. Later, analysis of atmospheric drag from Doppler data from the NAV team was also included. These analyses were presented to and reviewed by the larger group. Meetings included representatives from spacecraft mission operations and recommendations were made for adjustment of flyby altitudes for some of the early encounters.

Early on there was a strong effort to develop more accurate models for upper atmospheric densities. It was recognized that the atmospheric structure varied with latitude, local time, and perhaps longitude. The search for well-defined variations with these geophysical variables was ultimately unsuccessful because of the extreme variability of the atmosphere coupled with the sparse sampling afforded by the Titan flybys. Attempts in this direction are described, for example, in Westlake et al. (2011) and Snowden et al. (2013). However, patterns were not obvious initially. The issue was further clouded by the comparison of measurements made with different techniques that had not yet been intercalibrated. For example, the Huygens Atmospheric Structure Instrument (HASI) measurements at equatorial latitudes showed larger densities at a given altitude than INMS and AACS measurements at high latitudes made during the T5 encounter. This led to the development of models with a strong equatorial bulge. It is now clear that the density difference was due in part to a calibration difference (primarily with INMS) and in part due to the temporal variability of the atmosphere.

The first deep sampling of the Titan atmosphere occurred on T16, which penetrated to an altitude of 950 km where the density was $2.3 \times 10^{-9} \text{ kg m}^{-3}$, a transition regime with a Knudsen number of 1-10. At these high densities, the INMS measurements also became compromised by a high background caused by molecular collisions within the instrument. In other words, the mean free path between collisions became comparable to the instrument dimensions and this adversely affected the INMS mass filtering capabilities (Fig. 1). It also became clear that the most important scientific information could be obtained at somewhat smaller densities. Thus, the pressure to penetrate to the densities measured during T16 or deeper became less and the project settled in to a somewhat less aggressive approach toward minimum flyby altitudes.

Table 1: Duty Cycles and Maximum Densities

Pass	Minimum Altitude (km)	Thruster Duty Cycle	Measured Density (AACS) ($10^{-10} \text{ kg m}^{-3}$)
TA	1174	6%	2.04
TB	1192		
T5	1028	20%	6.36
T7	1075	14%	4.13
T16	950	62%	23.34
T17	1000	19%	7.62
T18	960	42%	16.78
T19	980	28%	10.60
T20	1030	44%	6.70
T21	1000	31%	11.10
T23	1000	28%	10.64
T25	1000	26%	8.24
T26	980	35%	11.49
T27	1010	36%	8.51
T28	990	41%	12.61
T29	980	51%	16.34
T30	960	54%	17.69
T32	965	54%	16.77
T36	973	33%	10.59
T39	970	46%	13.67
T40	1014	28%	8.09
T41	1010	41%	10.44
T42	999	27%	8.33
T43	1001	25%	7.70
T47	1023	16%	3.07
T48	960	42%	13.29
T49	970	37%	13.05
T50	967	48%	14.15
T51	963	44%	13.81
T55	966	44%	13.30
T56	968	34%	10.81
T57	955	69%	20.46
T58	965.8	43%	11.9
T59	956.2	43%	12.8
T61	960.7	51	15.71
T64	951.3	43	Some data missing
T65	1074	4	1.52

Table 1: continued

Pass	Minimum Altitude (km)	Thruster Duty Cycle	Measured Density (AACS) ($10^{-10} \text{ kg m}^{-3}$)
T70	878	50	39.8
T71	1005	27	7.66
T83	955	36.25	10.97
T84	959	29.1	9.09
T86	956	31	9.12
T87	973	27.58	5.1
T91	970	17.5	4.84
T92	964	34.39	10.4
T95	961	50.01	14.0
T100	963	25	7.3
T104	964	22.51	6.3
T106	1013	4.7	1.1
T107	980	20	6.2
T108	970	16.875	4.89
T113	1035	13.1	1.3
T117	971	13.125	2.14
T118	971	17.5	6.17
T119	975	37.5	4.91
T120	975	17.5	3.48
T121	976	29.38	7.17
T126	973	9.38	2.65

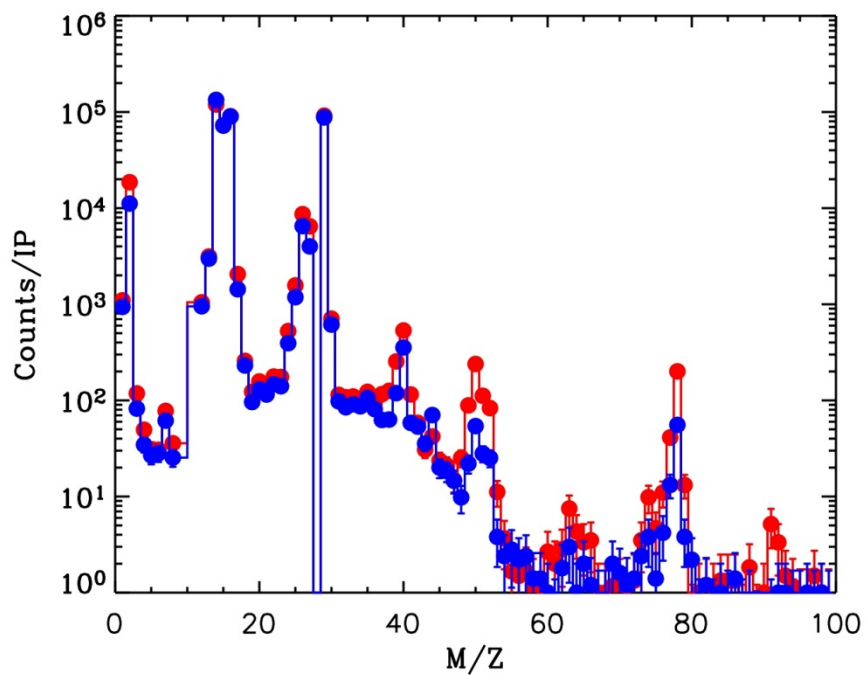


Fig 1. INMS mass spectra obtain during T16. Red is inbound, blue outbound. The high background below $m/z=50$ ($m/z=\text{mass}/\text{charge}$) is due to molecular scattering within the instrument.

Atmospheric Density Intercalibration

Titan atmospheric densities can be inferred from a variety of techniques using the Cassini orbiter data including analysis of measurements by the INMS (e.g. Cui et al., 2009 and Magee et al., 2009) and UVIS (e.g. Kammer et al., 2013) instruments, analysis of the thruster activity used to counteract atmospheric torque by the AACS, analysis of the spacecraft trajectory, and in rare instances, by analysis of orbiter accelerometer measurements. Additionally, atmospheric densities can be inferred from the accelerometer measurements included in the HASI suite. TAMWG examined all of these data sets and the initial results indicated a wide range of density values (Table 2). It therefore became paramount to establish consistent calibrations so that real atmospheric variations could be separated from differences due to instrument calibration.

Table 2: Early Titan Upper Atmospheric Densities Compared

Early Titan Upper Atmospheric Densities Compared (Ralph Lorenz 6/20/2018)

Instrument	Flyby	Date	Local			Density @1175km kg/m ³	Density @1025km kg/m ³	Density @950km kg/m ³	Source
			Latitude deg	Solar Time hr:min	Longitude * *				
INMS	TA	2004-300	38	16:45	-88	1.00E-10			Yelle/TAMWG *2.2 per Teolis
AACS	TA	2004-300	38	16:45	-88	1.80E-10			Sarani 2007
INMS	TB	2004-348	49	17:10	-81	7.50E-11			Yelle/TAMWG *2.2 per Teolis
UVIS	TB	2004-348	-36	23:00	40	1.00E-10	1.00E-09	3.60E-09	Yelle/TAMWG *2.2 per Teolis
HASI	TC	2005-014	-8.9	10:04	186	1.25E-10	7.43E-10	1.86E-09	HASI Level 4 Product on PDS
INMS	T5	2005-106	74	23:09	88	4.30E-11	3.00E-10	1.10E-09	Yelle/TAMWG *2.2 per Teolis
AACS	T5	2005-106	74	23:09	88	7.40E-11	6.00E-10	1.70E-09	Sarani 2007
AACS	T7	2005-250	-67	4:50		7.00E-11			Sarani 2007
UVIS	T10	2006-015	-60	20:04	5	6.83E-11			Derived** from Koskinen N2
AACS	T16	2006-203	85	2:24			6.00E-10	2.30E-09	Sarani 2007
UVIS	T21	2006-346				8.01E-11	6.36E-10	1.36E-09	Koskinen N2+CH4

* published values differ - NB in-situ values may sweep over a large lat/long/local time range
Similarly the area probed by an occultation will be different from that probed in-situ on the same flyby

** N2@1198km *1.02 (alt 1198->1175) *1.05 (N2 -> N2+CH4)

The thorniest issue was the relative calibration of INMS and AACS (see also Appendix 2). The densities derived from these two subsystems are coincident in space and time and therefore any differences had to be due to instrument calibration. AACS measured the mass density while INMS measured densities from individual species. Titan's upper atmosphere is composed primarily of N₂ and CH₄ and so adding the mass density from these two species together provides the atmospheric mass density, which can be directly compared to AACS results.

Derivation of atmospheric densities from AACS measurements is described in (Sarani 2007, 2009; Feldman et al., 2007; Lee and Lim, 2013; Andrade et al., 2015). The technique consists of using the torque experienced by the spacecraft, caused by its asymmetric shape and in particular the 11m magnetometer boom, to infer the atmospheric density. This depends critically upon the separation of the center of pressure and center of mass of the spacecraft. The center of pressure, of course, depends on spacecraft attitude. The offset of these two vectors was estimated from spacecraft CAD drawings, but it should be noted that some uncertainty in the center of mass existed, especially early in the mission, because the distribution of liquid fuel and oxidizer in the only partly-filled propellant tanks was not completely deterministic.

Operation of the INMS is described in Waite et al. (2004) and the most recent calibration in Teolis et al. (2015). The main uncertainties are due to detector degradation, which was difficult to measure accurately, and the complicated nature of the gas flow through the instrument. For all spacecraft mass spectrometers, the calibration is in part theoretical. The detector efficiency and gas conduction of the instrument can be measured pre-flight in the lab, but it is not possible to simulate spaceflight conditions in the lab. Cassini passed through Titan's atmosphere at a speed of ~ 6 km/sec and it is not possible to produce gas flow at this speed in a laboratory with a flux that enables calibration of a spaceflight mass spectrometer. Instead, INMS and past mass spectrometers have relied upon models for the flow of gas through the instrument at relevant speeds. Initially, the INMS calibration was based on analytic approximations describing this interaction. The disagreement between AACS and INMS densities spurred development of a Monte Carlo model for the instrument performance.

INMS neutral density measurements were made primarily in the Closed Source Neutral (CSN) mode in which atmospheric molecules are thermalized in an antechamber, before migrating through a coupling conduit to the ionization chamber. The Monte Carlo model consists of tracing the trajectories of individual molecules as they interact with the antechamber and the conduit. The model is quite complicated and cannot be described fully here and the interested reader is referred to the paper by Teolis et al. (2015). The model was partly validated through a series of in-flight experiments. These consisted of predicting the INMS response to various spacecraft attitudes in different environments, comparison of the model predictions with the measured response, then adjustment of model parameters, essentially components of the instrument conductance, to best match the measurements. The model and calibration experiments are described in detail in Teolis et al. (2015).

Although the Monte Carlo model is quite sophisticated some of the input parameters are unknown. The model depends upon simple assumptions for the interaction of atmospheric molecules with metal surfaces. Data on the scattering of molecules off instrument surfaces is lacking and the model assumes complete thermalization during a collision. This is unlikely to be rigorously correct but there is insufficient data for a more accurate treatment. We note that the value of the drag coefficient used in the AACS analysis also assumes that molecular velocities are thermalized upon collision and diffusively reflected.

The Monte Carlo model for the instrument performance differed significantly from the analytic approximation used previously and brought the INMS results closer to the AACS results, but did not rectify the two sets of measurements. Additionally, it was assumed that the INMS detector suffered a sensitivity decrease by a factor of 1.55. This level of decrease is typical for a Channeltron electron multiplier; however, the direct evidence for it is not strong. The argument for adjusting the INMS calibration to match the AACS results is that the AACS is a much simpler system.

Figs. 2a and 2b show a comparison of INMS and AACS density measurements for 35 low altitude passes through Titan's atmosphere using the Teolis et al. (2015) calibration. Overall, the agreement is quite good. Densities at closest approach usually match quite well. In some cases, differences develop at higher altitudes. These differences are not understood, but, in this regime, preference should be given to the INMS data as the aerodynamic torques are becoming small and AACS' ability to detect small torques is accompanied with large errors. Additionally, it is well established that the INMS has a linear and repeatable response to atmospheric density.

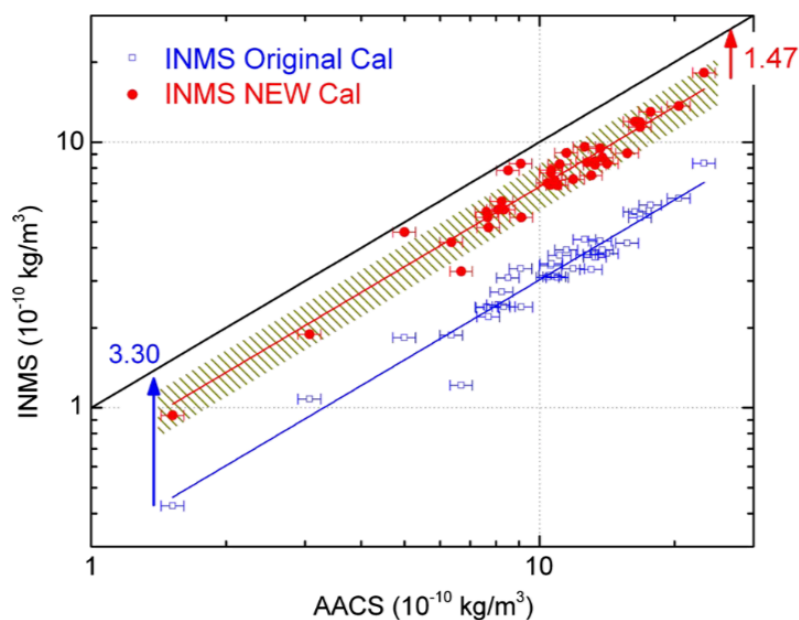


Fig. 7 Comparison of INMS and AACS Titan closest approach densities for multiple flybys, and the INMS/AACS ratio fit, with the original and new INMS calibration models. *Error bars* show the AACS $\pm 5.8\%$ (Feldman et al. 2007) 1σ random (measurement) error. The INMS random errors bars in the range 0.02–0.1 % are not visible on this scale. The error of the ratio is dominated by the systematic (modeling) error of both systems. The INMS systematic error of $\pm 23\%$ (i.e., the range by which all the points could be plausibly shifted vertically together) is shown by the *hashed region* to distinguish from random error. The hashed region does not encompass the 1.0 ratio line, and therefore the INMS systematic error is insufficient by itself to account for the 1.47 ratio with AACS

Fig. 2a. Comparison of INMS and AACS density measurements in the form of a scatter plot (from Teolis et al., 2015).

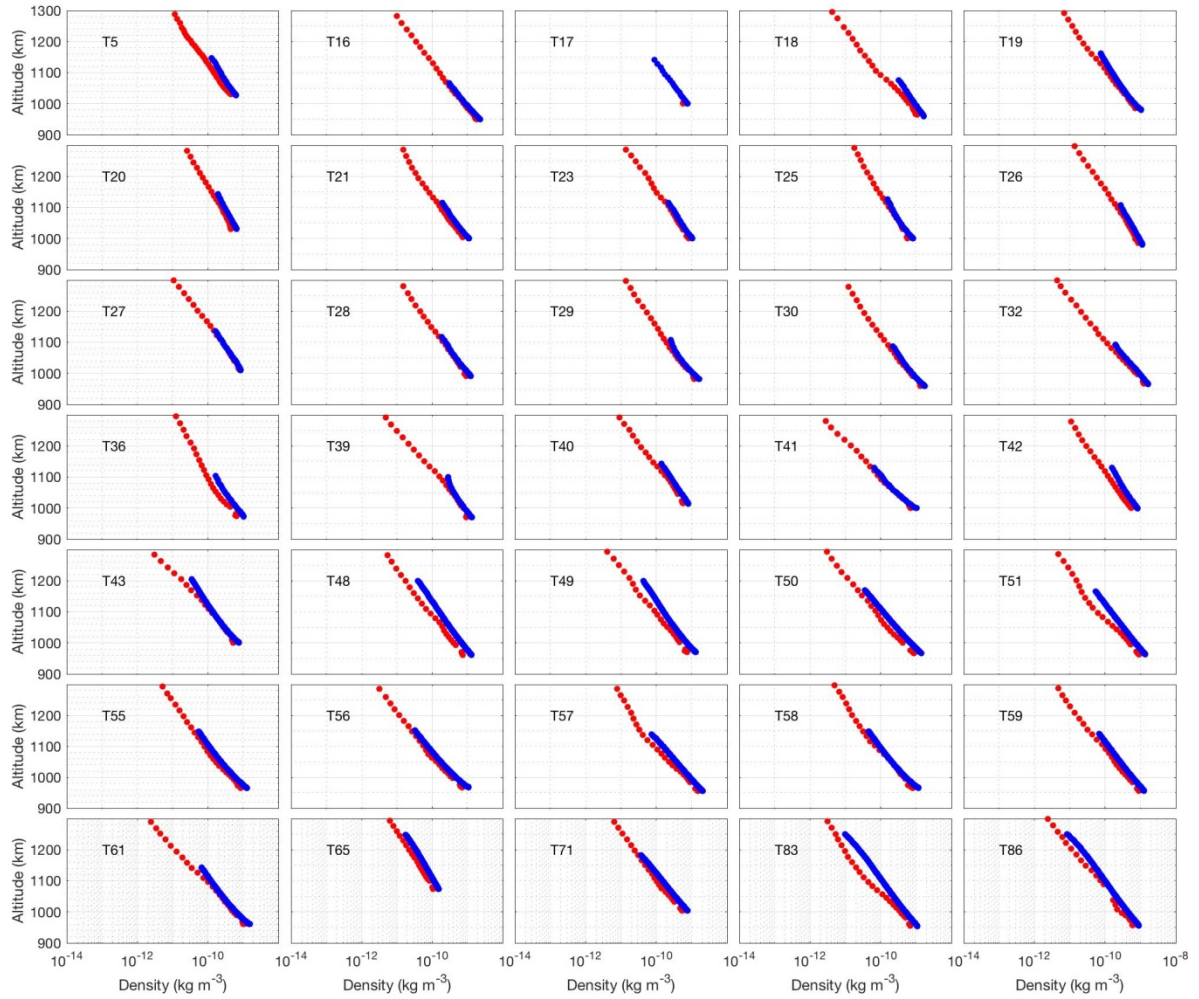


Fig. 2b. Comparison of INMS (red) and AACS (blue) density measurements for 35 Titan passes.

T87 and T107

In order to investigate further the discrepancy between the INMS and AACS results, flybys T87 and T107 were designed to optimize measurements of density derived from the spacecraft tracking information provided by the NAV team and from thrusting accelerations measured by the on-board accelerometer, which is normally used for Main Engine maneuvers (Pelletier et al., 2006; Roth et al., 2008; Boone 2015). These measurements require substantial periods of two-way Doppler tracking and, even so, the derived densities have significant random components. However, the measurements have smaller systematic uncertainties than other techniques. Results depend primarily on the spacecraft projected area and drag coefficient whereas the densities derived from the AACS torque measurements also depend on the vector from the center of mass to the center of pressure. The NAV and acceleration measurements remove any uncertainty due to possible errors in our knowledge of this vector.

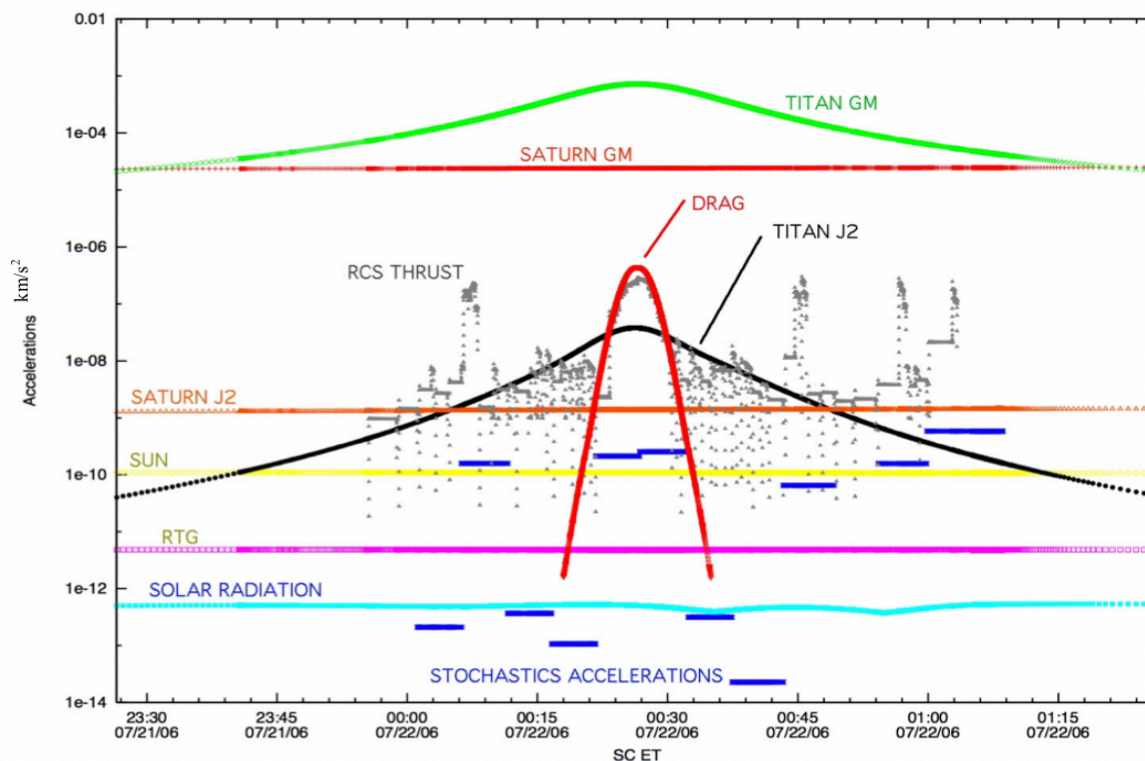


Fig. 3. Components of accelerations experienced by Cassini during the T16 flyby of Titan which reached an altitude of 949.9km. The atmospheric drag is easily separated from the gravity and thruster accelerations (Boone 2015).

The NAV analysis consists of determining the deceleration of the spacecraft due to atmospheric drag. This requires removal of other similar sources of acceleration, primarily acceleration due to the spacecraft thrusters and due to the J2 components of the gravity field of Titan. Fortunately, as shown in Fig. 3, the time signatures of these three forces are quite different

allowing confident removal of the gravity and thruster accelerations to isolate atmospheric drag.

Results of the analysis are shown in Fig. 4, which also compares the derived densities with INMS densities using the Teolis et al. (2015) calibration. The results from both T87 and T107 support the AACS-derived densities and the revised INMS calibration.

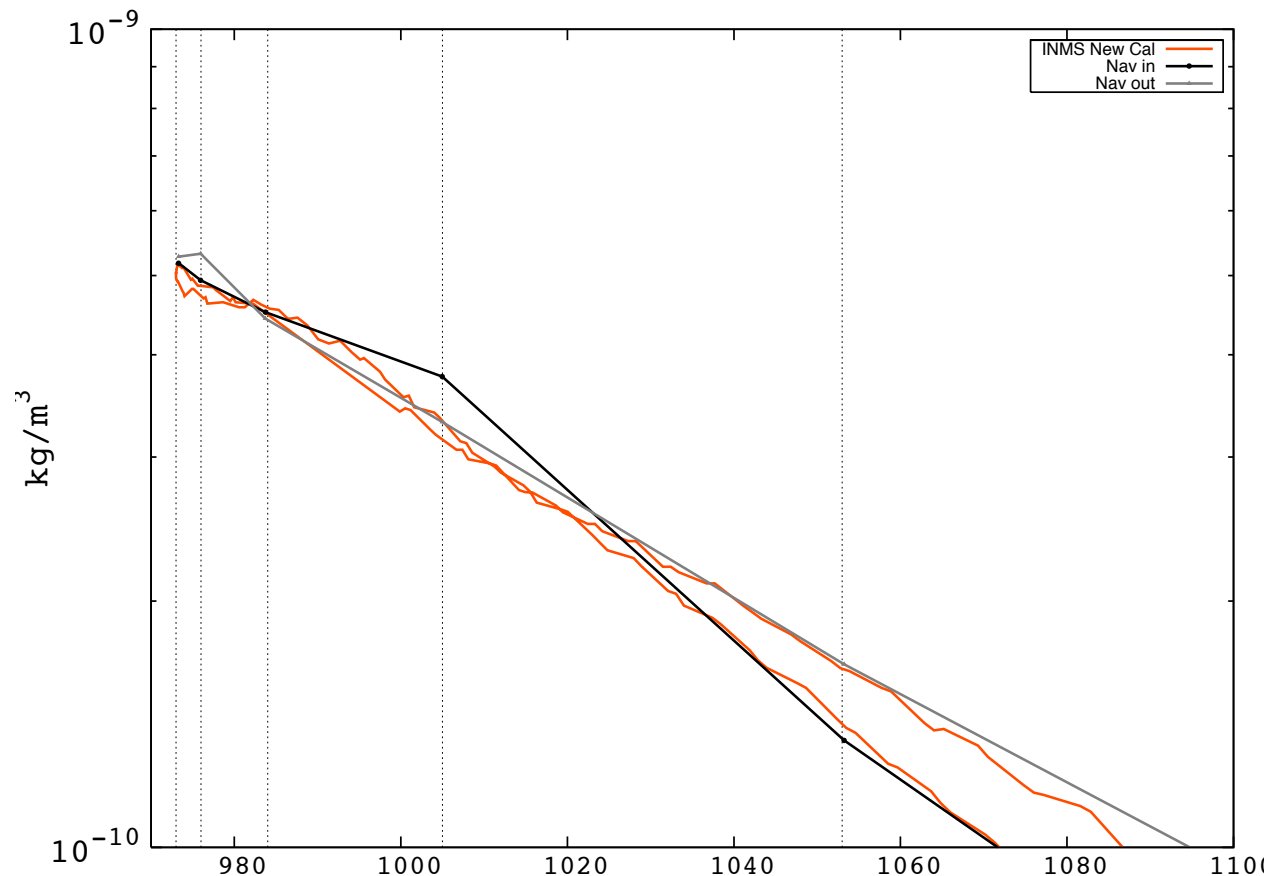


Fig. 4. Comparison of T87 atmospheric densities determined from NAV spacecraft tracking with those derived from INMS measurements using the Teolis et al. (2015) calibration (INMS New Calibration).

In addition to the comparison with NAV, the T87 measurement provided an opportunity for a more detailed comparison of INMS and AACS results. In order to smooth the noisy angular momentum data, the AACS team fit the data with a hyperbolic tangent function versus time from closest approach (Sarani 2009). This forces symmetric results for the inbound and outbound legs of the trajectory. The derived density therefore should be viewed as an average of inbound and outbound. For T87, a separate analysis was performed by Yelle that dispensed with the assumption of inbound/outbound symmetry. Instead, the AACS measurements of accumulated momentum were smoothed with a Savitsky-Golay filter (Savitzky and Golay, 1964) using a polynomial of degree 2 for a span of 11 points. Densities derived with this technique are in excellent agreement with the INMS densities (Fig. 5). This suggests that differences between INMS and AACS results in Fig. 4 could be due to the assumption of inbound/outbound asymmetry.

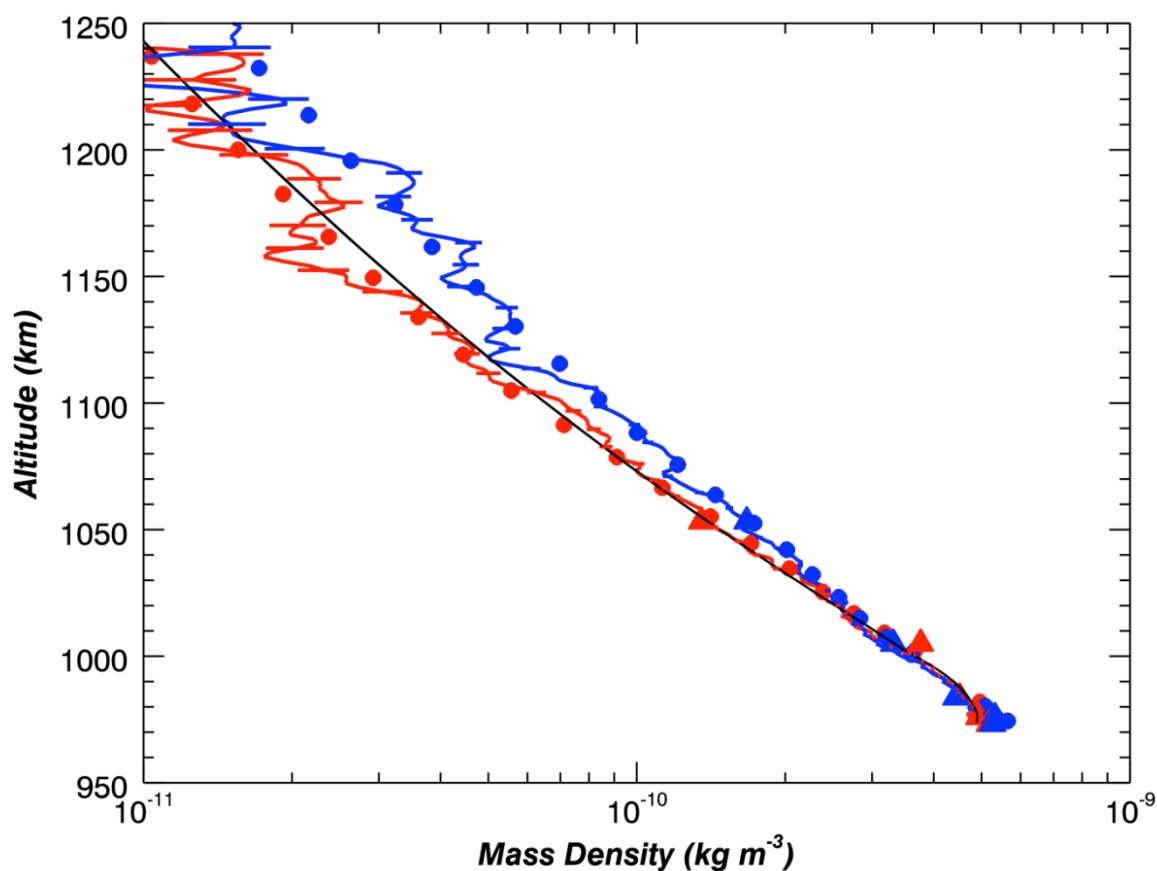


Fig. 5. Comparison of INMS and AACS T87 densities (red are inbound and blue are outbound). Filled circles are INMS densities, while solid lines are densities derived by Yelle from AACS measurements.

UVIS Occultations

The densities of Titan's upper atmosphere have been determined from measurements of UV stellar and solar occultations of Titan. Only occultations in the EUV can determine the N₂ density as N₂ does not absorb significantly longward of 100 nm. Solar EUV occultations measure absorption in the photo-ionization region, shortward of 80 nm, where the N₂ cross section varies smoothly with wavelength below ~65nm. Stellar occultations measure absorption in the 91-100 nm region where the N₂ cross section is highly structured. Because of interstellar absorption, there is no measurable stellar flux shortward of 91 nm. UVIS observed stellar and solar occultations by Titan throughout the mission. To date, 9 solar and 5 stellar have been analyzed and are summarized in Table 3. Except for T118, the analysis of the solar occultations can be found in Capalbo et al. (2015). The T118 occultation has been analyzed by Yelle (presented in the next section). Analysis of the stellar EUV occultations are presented in Kammer et al. (2013).

Table 3: Occultation Measurements

Object	pass	Year	DOY	Latitude	Longitude	Local Time
Sun	T10	2006	15	-62, -54	0-11	20:04
Sun	T26	2007	69	-76, -77	41-29	23:10
Sun	T53	2009	110	-21, -29	237	18:03
Sun	T58	2009	189	87, 85	240-237	17:40
Sun	T62i	2009	285	2, -5	230	06:08
Sun	T62e	2009	285	-68, -61	48-49	17:59
Sun	T78i	2011	255	28, 32	162-161	05:41
Sun	T78e	2011	255	25, 20	354-352	18:25
Sun	T118i	2016	96			
Sun	T118e	2016	96			
Star		2006	346	35	116	
Star		2007	243	35	329	
Star		2008	54	4,24	333-173	
Star		2014	201			
Star		2014	265			

Densities inferred from occultation measurements are independent of instrument calibration because the analysis depends on the ratio of attenuated flux to the flux measured outside the atmosphere. As long as the instrument is stable over the time period of the measurement, typically minutes in duration, the measured ratio is independent of calibration. This removes a significant uncertainty from the analysis and the occultation results should be viewed as having high accuracy. This is especially true for the solar occultation which measure absorption in the N₂ ionization continuum because these cross sections are well known, with a typical accuracy of ~10% (Capalbo et al., 2015).

T118

A further experiment to aid in intercalibration of instruments was performed on T118. A solar occultation observation was scheduled fairly close to the location of the minimum altitude point in the trajectory, allowing a better comparison of occultation and in situ measurements than had been possible previously. The geometry of the experiment is shown in Fig. 6.

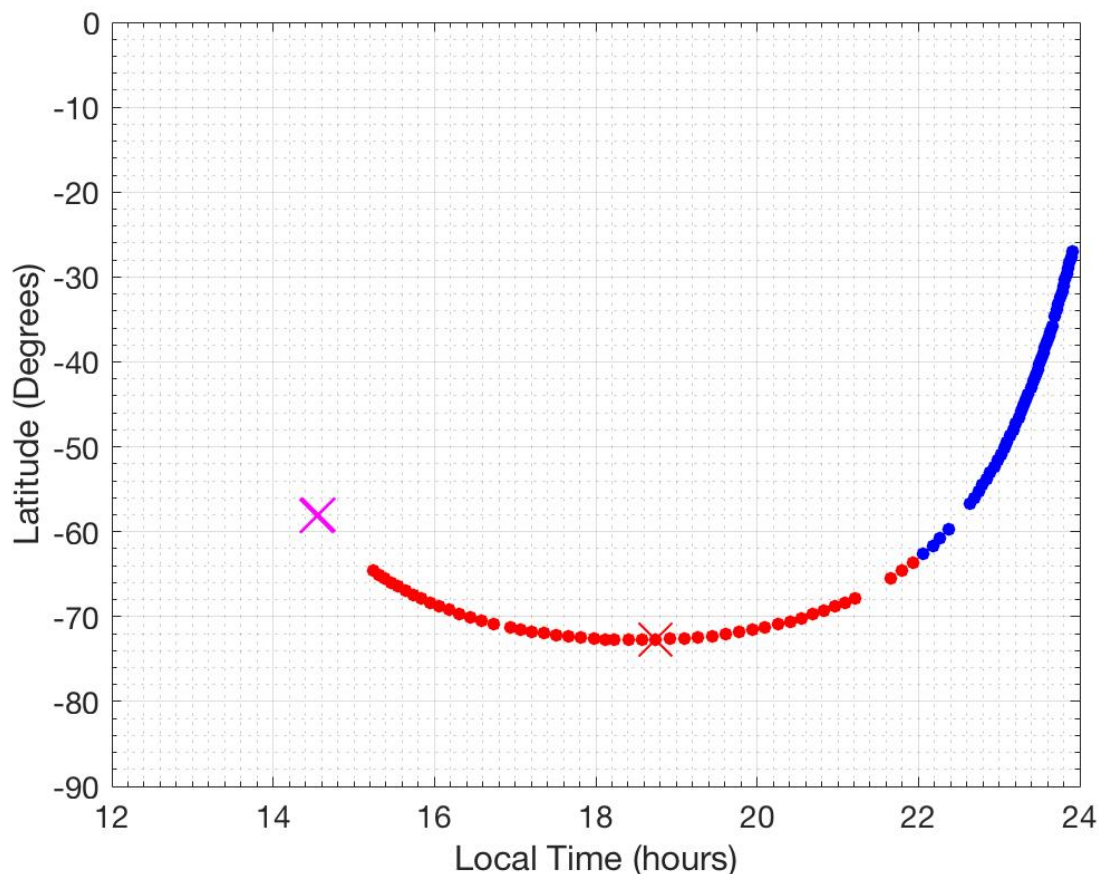


Fig. 6. Geometry of the T118 Occultation and INMS/AACS in situ measurements. Circles show the spacecraft trajectory with inbound red and outbound blue. The magenta cross shows the location of the UVIS solar occultations. The red cross shows the location of the in-situ measurements at the altitudes that overlap with the occultation.

Densities from both data sets are shown in Fig. 7. The INMS, AACS, and UVIS measurements probe the atmosphere in different altitude regions. UVIS is sensitive to lower densities at high altitude and AACS to higher densities at low altitudes. INMS has a larger dynamic range than the other measurements over the altitude ranges for the other experiments. As can be seen in the figure, there is good agreement among the different measurements, especially considering that the occultation was located several hours of local time and ~ 10 degrees in latitude from the in-situ measurements.

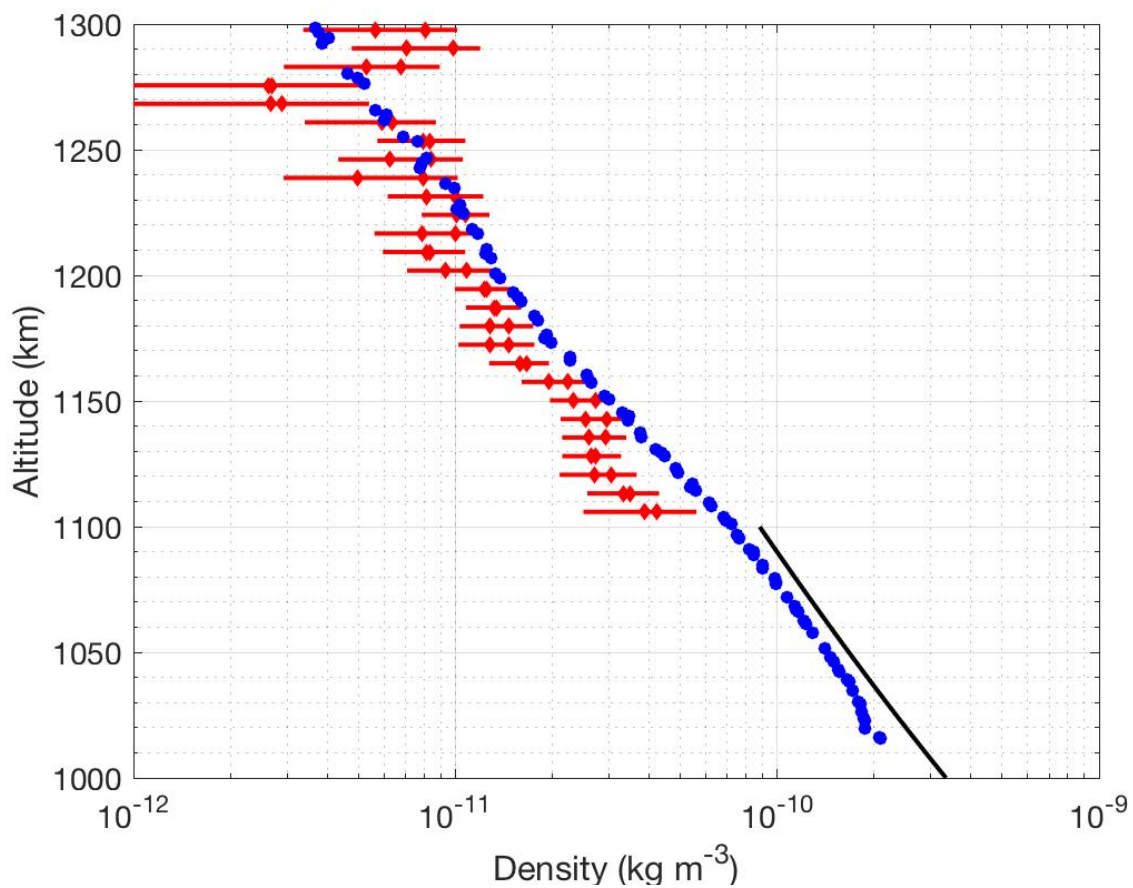


Fig. 7. Comparison of densities from T118. The black line represents AACS densities, the blue points INMS densities, and the red points UVIS solar occultation densities.

Summary

Fig. 8 presents a summary of INMS and occultation measurements of Titan's upper atmospheric density profile. We do not include AACS densities in this comparison because it has been shown in Figs. 4 and 5 that they agree with INMS, while the INMS densities cover a broader altitude range with better defined random uncertainties. Also included in the figure is the HASI density profile and densities from occultation measurements. There are several noteworthy features. First, the atmosphere is highly variable. The density variability is a factor of 3 at the lowest altitudes, rising to more than a factor of 10 near 1300 km. Second, the occultation and INMS results are consistent in the sense that they do not exhibit a systematic difference that is detectable, given the level of variability. Third, the HASI profile is at the upper end of the range densities, but is not beyond that range. For example, the T10 solar occultation and the T100 INMS density measurements are both comparable to the HASI measurements. It is therefore reasonable to conclude that there is no calibration difference between the HASI and INMS, and the Huygens probe simply entered a region of high density in the upper atmosphere.

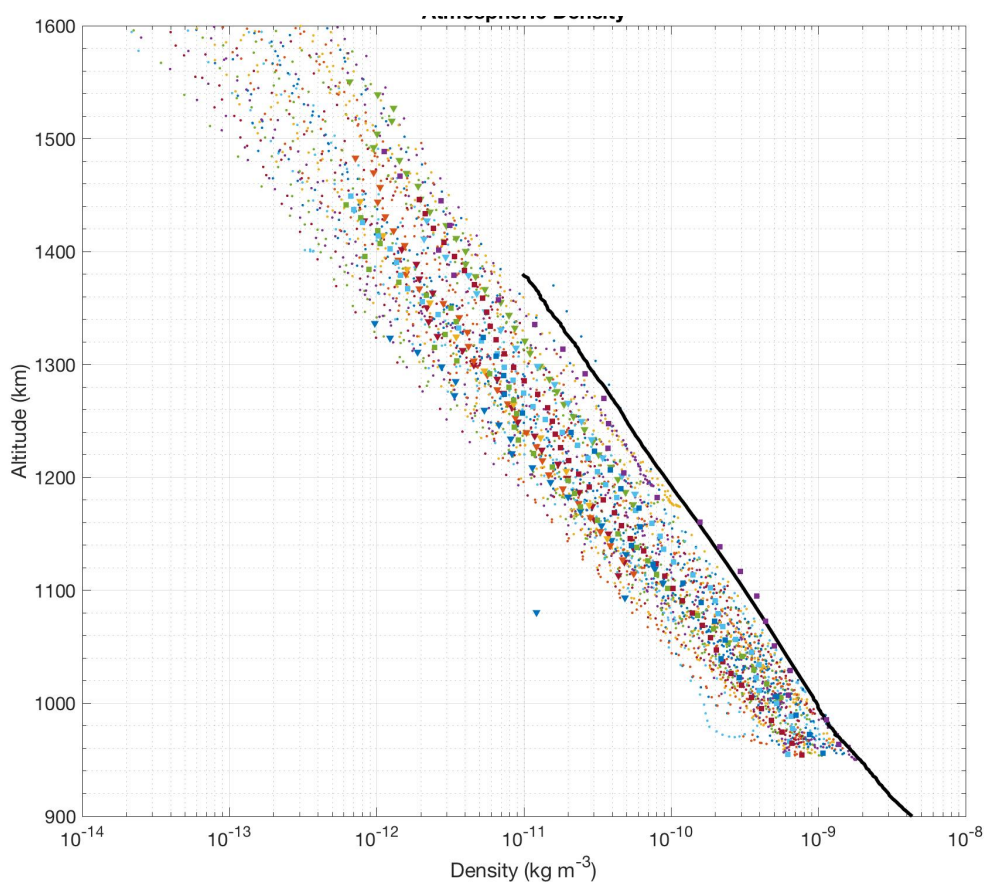


Fig. 8. Comparison of density profiles measured during the Cassini mission. Dots represent INMS measurements, triangles occultation measurements, squares occultation measurements. The solid black line is the HASI density profile.

In this connection, it may be noted that there is good correspondence (when the new INMS recalibration is considered) between the various orbiter measurements taken in the first few flybys of the mission in 2004-2005, and the HASI profile in early 2005. Orbiter data after 2007-2009 at a given altitude generally indicates lower densities than in 2004-2005. Although a full empirical model of the deterministic variations of Titan upper atmosphere densities has not been developed, this trend is fully consistent with the systematic decline both of total insolation 2003-2017 due to Titan's receding from the sun due to Saturn's orbital eccentricity, and of ultraviolet flux due to the solar cycle. These effects are shown in Figs. 9 and 10.

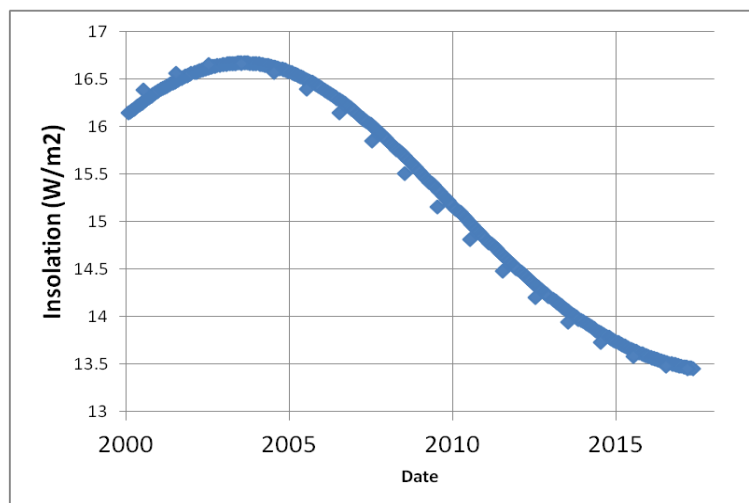


Fig. 9. Top-of-Atmosphere Solar Flux as a function of date. The flux drops by $\sim 18\%$ over the nearly half-Titan-year of the mission, due to Saturn's orbital eccentricity of 0.09, changing the Sun-Titan distance by about 1 AU.

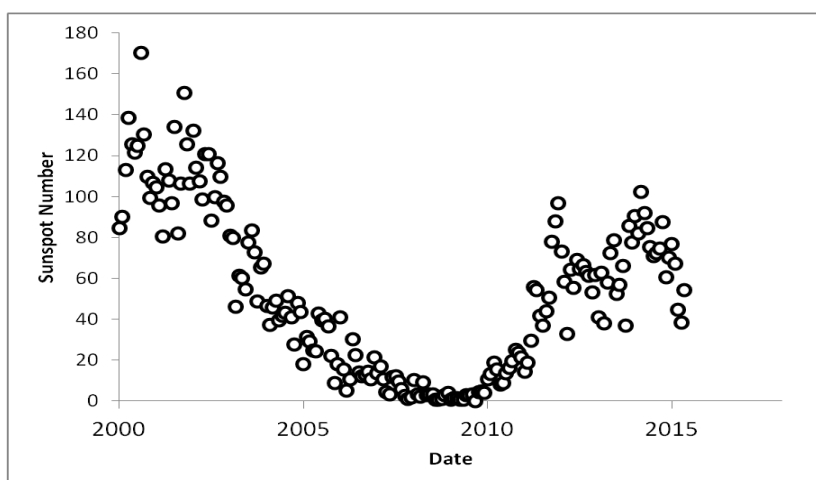


Fig. 10. The sunspot number, a proxy for ultraviolet flux which heats Titan's atmosphere above about 1000km. The flux is declining between 2004 and 2009, leading to contraction of the upper atmosphere and thus declining densities at a given altitude.

Lastly, Fig. 8 clearly illustrates the variability of atmospheric density. There are two important, but separate points. The variability extends to the bottom of the atmosphere, where the variability is about a factor of 3. In addition, the variability increases with increasing altitude. This indicates that the temperatures in the upper atmosphere also vary widely. This has been discussed extensively in Snowden et al. (2013) and Waite et al. (2013). Using the techniques described in Snowden et al. (2013), temperature profiles have been generated from INMS measurements for each low altitude pass. The mean temperature and standard deviation of this set of temperature profiles is shown in Fig. 11. The mean is roughly constant with altitude at 150 K with a standard deviation of ~ 25 K.

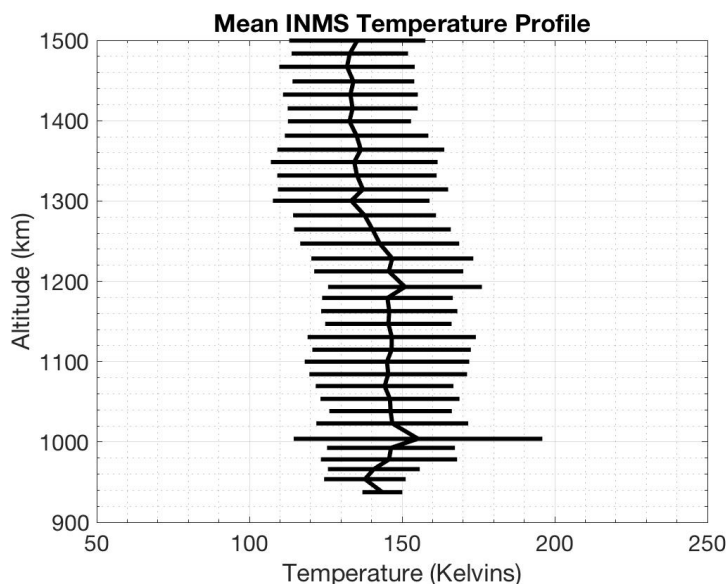


Fig. 11. Mean temperature profile for all low altitude flybys and its standard deviation.

Cassini's exploration of Titan has led to remarkable discoveries that deserve further exploration. Cassini science and engineering data can be found in the Planetary Data Archive (https://pds-atmospheres.nmsu.edu/data_and_services/atmospheres_data/Cassini/sci-titan.html#finding-data). Already missions are being proposed and developed to send landers, aircraft, and orbiters back to this Earth-like, possibly habitable, outer solar system moon. We hope that this report will help to illustrate the complexities involved with a variable, seasonally changing atmosphere.

References

- Andrade, L.C., Burk, T.A., and Pelletier, F., "Titan Density Reconstruction Using Radiometric and Cassini Attitude Control Flight Data," AIAA SciTech, Kissimmee, Florida, Paper AIAA 2015-0079, AIAA Guidance, Navigation, and Control Conference, 5–9 January 2015.
<https://doi.org/10.2514/6.2015-0079>
- Boone, D.R. "Titan Atmospheric Density Results From Cassini's T107 Flyby". 25th International Symposium on Space Flight Dynamics, October 19 – 23, 2015, Munich, Germany. #108.
https://issfd.org/2015/files/downloads/papers/108_Boone.pdf
- Capalbo, Fernando J.; Bénilan, Yves; Yelle, Roger V.; Koskinen, Tommi T., 2015. "Titan's Upper Atmosphere from Cassini/UVIS Solar Occultations". The Astrophysical Journal, Volume 814, Issue 2, article id. 86, 14 pp. DOI:10.1088/0004-637X/814/2/86
- Courtin, R., Gautier, D., McKay, C.P., 1995. "Titan's thermal emission spectrum: reanalysis of the Voyager infrared measurements". Icarus 114, 144–162. DOI:10.1006/icar.1995.1050
- Cui, J.; Yelle, R. V.; Vuitton, V.; Waite, J. H.; Kasprzak, W. T.; Gell, D. A.; Niemann, H. B.; Müller-Wodarg, I. C. F.; Borggren, N.; Fletcher, G. G.; Patrick, E. L.; Raaen, E.; Magee, B. A., 2009. "Analysis of Titan's neutral upper atmosphere from Cassini Ion Neutral Mass Spectrometer measurements". Icarus, Volume 200, Issue 2, p. 581-615. DOI:10.1016/j.icarus.2008.12.005
- Feldman, A., Brown, J.M., Wang, E.K., Peer, S.G., and Lee, A.Y., "Reconstruction of Titan Atmosphere Density Using Cassini Attitude Control Flight Data". Proceedings of the 17th AAS/AIAA Space Flight Mechanics Meeting, American Astronomical Society Paper 07-187, Feb. 2007. Paper AAS07-187
- Hubbard, W. B.; Sicardy, B.; Miles, R.; Hollis, A. J.; Forrest, R. W.; Nicolson, I. K. M.; Appleby, G.; Beisker, W.; Bittner, C.; Bode, H. -J.; Bruns, M.; Denzau, H.; Nezel, M.; Riedel, E.; Struckmann, H.; Arlot, J. E.; Roques, F.; Sevre, F.; Thuillot, W.; Hoffmann, M. Geyer, E. H.; Buil, C.; Colas, F.; Lecacheux, J.; Klotz, A.; Thouvenot, E.; Vidal, J. L.; Carreira, E.; Rossi, F.; Blanco, C.; Cristaldi, S.; Nevo, Y.; Reitsema, H. J.; Brosch, N.; Cernis, K.; Zdanavicius, K.; Wasserman, L. H.; Hunten, D. M.; Gautier, D.; Lellouch, E.; Yelle, R. V.; Rizk, B.; Flasar, F. M.; Porco, C. C.; Toubanc, D.; Corugedo, G., 1993. "The occultation of 28 SGR by Titan." Astronomy and Astrophysics, Vol. 269, p. 541-563.
- Kammer, J. A.; Shemansky, D. E.; Zhang, X.; Yung, Y. L., 2013. "Composition of Titan's upper atmosphere from Cassini UVIS EUV stellar occultations". Planetary and Space Science, Volume 88, p. 86-92. DOI:10.1016/j.pss.2013.08.003
- Lee, A.Y. and Lim, Ryan S., "Evidence of Temporal Variation of Titan Atmospheric Density in 2005–2013," AIAA-2013-4709, Proceedings of the AIAA Guidance, Navigation, and Control Conference, Boston, Massachusetts, August 19–22, 2013. DOI: 10.2514/6.2013-4709.
<https://doi.org/10.2514/6.2013-4709> and <https://ntrs.nasa.gov/search.jsp?R=20150008682>
- Lellouch, E., Bezaud, B., Flasar, F.M., Vinatier, S., Achterberg, R., Nixon, C.A., Bjoraker, G.L., Gorius, N., 2014. The distribution of methane in Titan's stratosphere from Cassini/CIRS observations. Icarus 231, 323–337. DOI:10.1016/j.icarus.2013.12.016
- Lindal, G. F.; Wood, G. E.; Hotz, H. B.; Sweetnam, D. N.; Eshleman, V. R.; Tyler, G. L., 1983. "The atmosphere of Titan: An analysis of the Voyager 1 radio occultation measurements". Icarus, Volume 53, Issue 2, p. 348-363. DOI: 10.1016/0019-1035(83)90155-0
- Magee, Brian A.; Waite, J. Hunter; Mandt, Kathleen E.; Westlake, Joseph; Bell, Jared; Gell, David A., 2009. "INMS-derived composition of Titan's upper atmosphere: Analysis methods and model comparison". Planetary and Space Science, Volume 57, Issue 14-15, p. 1895-1916. DOI:10.1016/j.pss.2009.06.016

- Mori, Koji; Tsunemi, Hiroshi; Katayama, Haruyoshi; Burrows, David N.; Garmire, Gordon P.; Metzger, Albert E., 2004. "An X-Ray Measurement of Titan's Atmospheric Extent from Its Transit of the Crab Nebula". *The Astrophysical Journal*, Volume 607, Issue 2, pp. 1065-1069. DOI:10.1086/383521
- Niemann, H. B.; Atreya, S. K.; Demick, J. E.; Gautier, D.; Haberman, J. A.; Harpold, D. N.; Kasprzak, W. T.; Lunine, J. I.; Owen, T. C.; Raulin, F., 2010. "Composition of Titan's lower atmosphere and simple surface volatiles as measured by the Cassini-Huygens probe gas chromatograph mass spectrometer experiment". *Journal of Geophysical Research*, Volume 115, Issue E12, CitelD E12006. DOI: 10.1029/2010JE003659
- Pelletier, F. J.; Antreasian, P. G.; Bordi, J. J.; Criddle, K. E.; Ionasescu, R.; Jacobson, R. A.; Mackenzie, R. A.; Parcher, D. W.; Stauch, J. R. "Atmospheric drag model for Cassini orbit determination during low altitude Titan flybys". 16th AAS/AIAA Space Flight Mechanics Conference, Tampa, Florida, January 22-26, 2006. Paper AAS 06-141. <https://ntrs.nasa.gov/search.jsp?R=20060043676>
- Roth, Duane C.; Antreasian, Peter G.; Ardalan, Shadan M.; Criddle, Kevin E.; Goodson, Troy; Ionasescu, Rodica; Jones, Jeremy B.; Parcher, Daniel W.; Pelletier, Frederic J.; Thompson, Paul F.; Vaughan, Andrew T., 2008. "Navigational use of Cassini ΔV telemetry". AIAA/AAS Astrodynamics Specialist Conference, Honolulu, Hawaii, August 18-21, 2008. <https://doi.org/10.2514/6.2008-6746>
- Sarani, S., "Assessment of Per-axis Thruster Control Authority of Cassini Spacecraft for Low-altitude Titan Flybys," Paper AAS 04-275, Proceedings of the 14th AAS/AIAA Space Flight Mechanics Conference, Maui, Hawaii, pp. 2743–2766, February 8-12, 2004. <https://trs.jpl.nasa.gov/handle/2014/38021>
- Sarani, S., "A Novel Technique for the Reconstruction of Titan Atmospheric Density using Cassini Guidance, Navigation, and Control Data," AIAA-2007-6343, AIAA Guidance, Navigation, and Control Conference, Hilton Head, South Carolina, 20–23 August 2007. <https://doi.org/10.2514/6.2007-6343>
- Sarani, S., "Titan Atmospheric Density Reconstruction Using Cassini Guidance, Navigation, and Control Data," AIAA-2009-5763, AIAA Guidance, Navigation, and Control Conference, Chicago, Illinois, 10–13 August 2009. <https://doi.org/10.2514/6.2009-5763>
- Savitzky, A. and Golay, M.J.E., 1964. "Smoothing and Differentiation of Data by Simplified Least Squares Procedures". *Analytical Chemistry*. 36 (8): 1627–39. DOI:10.1021/ac60214a047.
- Seal, D. and Bittner, M., 2017. The epic chronicle of designing Cassini's Titan flyby altitudes. Paper presented at the IEEE Aerospace Conference, Big Sky, Montana, March 2013. DOI:10.1109/AERO.2017.7943848
- Sicardy, B.; Ferri, F.; Roques, F.; Lecacheux, J.; Pau, S.; Brosch, N.; Nevo, Y.; Hubbard, W. B.; Reitsema, H. J.; Blanco, C.; Carreira, E.; Beisker, W.; Bittner, C.; Bode, H. -J.; Bruns, M.; Denzau, H.; Nezel, M.; Riedel, E.; Struckmann, H.; Appleby, G. Forrest, R. W.; Nicolson, I. K. M.; Hollis, A. J.; Miles, R., 1999. "The Structure of Titan's Stratosphere from the 28 Sgr Occultation". *Icarus*, Volume 142, Issue 2, pp. 357-390. DOI:10.1006/icar.1999.6219
- Smith, G. R.; Strobel, D. F.; Broadfoot, A. L.; Sandel, B. R.; Shemansky, D. E.; Holberg, J. B., 1982. "Titan's upper atmosphere: composition and temperature from the EUV solar occultation results". *Journal of Geophysical Research*, Volume 87, Issue A3, p. 1351-1360. DOI:10.1029/JA087iA03p01351
- Snowden, D.; Yelle, R. V.; Cui, J.; Wahlund, J. -E.; Edberg, N. J. T.; Ågren, K., 2013. "The thermal structure of Titan's upper atmosphere, I: Temperature profiles from Cassini INMS observations". *Icarus*, Volume 226, Issue 1, p. 552-582. DOI:10.1016/j.icarus.2013.06.006
- Strobel, D.F. and Sicardy, B., 1997 in Wilson(ed.) "Gravity Wave and Shear Models", In *Huygens: Science, Payload, and Mission*. ESA Publications Division, ESTEC, Noordwijk, The Netherlands, ESA SP 1177, pp. 299-312.

- Strobel, D. F.; Hall, D. T.; Zhu, X.; Summers, M. E., 1993. "Upper Limit on Titan's Atmospheric Argon Abundance". *Icarus*, Volume 103, Issue 2, p. 333-336. DOI: 10.1006/icar.1993.1075
- Teolis, B. D.; Niemann, H. B.; Waite, J. H.; Gell, D. A.; Perryman, R. S.; Kasprzak, W. T.; Mandt, K. E.; Yelle, R. V.; Lee, A. Y.; Pelletier, F. J.; Miller, G. P.; Young, D. T.; Bell, J. M.; Magee, B. A.; Patrick, E. L.; Grimes, J.; Fletcher, G. G.; Vuitton, V., 2015. "A Revised Sensitivity Model for Cassini INMS: Results at Titan". *Space Science Reviews*, Volume 190, Issue 1-4, pp. 47-84. DOI:10.1007/s11214-014-0133-8
- Vervack, Ronald J.; Sandel, Bill R.; Strobel, Darrell F., 2004. "New perspectives on Titan's upper atmosphere from a reanalysis of the Voyager 1 UVS solar occultations". *Icarus*, Volume 170, Issue 1, p. 91-112. DOI:10.1016/j.icarus.2004.03.005
- Waite, J. H.; Lewis, W. S.; Kasprzak, W. T.; Anicich, V. G.; Block, B. P.; Cravens, T. E.; Fletcher, G. G.; Ip, W. -H.; Luhmann, J. G.; McNutt, R. L.; Niemann, H. B.; Parejko, J. K.; Richards, J. E.; Thorpe, R. L.; Walter, E. M.; Yelle, R. V., 2004. "The Cassini Ion and Neutral Mass Spectrometer (INMS) Investigation". *Space Science Reviews*, Volume 114, Issue 1-4, pp. 113-231. DOI:10.1007/s11214-004-1408-2
- Waite, J. H.; Bell, J.; Lorenz, R.; Achterberg, R.; Flasar, F. M., 2013. "A model of variability in Titan's atmospheric structure". *Planetary and Space Science*, Volume 86, p. 45-56. DOI:10.1016/j.pss.2013.05.018
- Westlake, J. H.; Bell, J. M.; Waite, J. H., Jr.; Johnson, R. E.; Luhmann, J. G.; Mandt, K. E.; Magee, B. A.; Rymer, A. M., 2011. "Titan's thermospheric response to various plasma environments". *Journal of Geophysical Research: Space Physics*, Volume 116, Issue A3, CiteID A03318. DOI:10.1029/2010JA016251
- Yelle, R.V., Strobel, D.F., Lellouch, E., Gautier, D., 1997. "The Yelle Titan Atmosphere Engineering Models". *Huygens: Science, Payload and Mission, Proceedings of an ESA conference*. Edited by A. Wilson (1997)., p.243
- Yelle, Roger V.; Borggren, N.; de la Haye, V.; Kasprzak, W. T.; Niemann, H. B.; Müller-Wodarg, I.; Waite, J. H., 2006. "The vertical structure of Titan's upper atmosphere from Cassini Ion Neutral Mass Spectrometer measurements." *Icarus*, Volume 182, Issue 2, p. 567-576. DOI:10.1016/j.icarus.2005.10.029

Appendix 1: Safe Flyby Altitude for T7

D.F. Strobel (July 2005)

Response to Summary of 30 June 2005 TAMWG Telecon

I would like to advocate a substantially different approach to determining the appropriate T7 flyby altitude, in part because I do not trust probabilities from small data sets. We have six sets of data to work with: AACS (TA, T5), INMS (TA, T5), HASI (TC), and UVIS (TB). What is important is the maximum atmospheric torque that the thrusters can counterbalance. Thus the only useful data sets are those for which we have mass density measurements and thruster firing rates. Consequently, HASI and UVIS data sets are not relevant.

Because we still do not understand why AACS and INMS mass densities differ by \sim factors of 2-4, we should regard these measurements as relative density measurements, but their height profiles as accurate (assuming that the atmosphere is locally spherically symmetric). That is, the density variation as a function of altitude is accurate, but the overall profile may need to be multiplied by a to-be-determined factor in either or both cases. (As part of the report, we should put together plots of the mass density profiles for AACS and INMS on TA and T5, so we can get a better idea of how well their profiles agree in shape.)

How do we determine flyby altitude for T7? One approach is to use the tumble density as the basis. For T3, the tumble density was calculated to be $19.15 \times 10^{-10} \text{ kg m}^{-3}$ ("Loss of Control Authority" Titan Density During 950-km Titan Flyby Allan Y. Lee and David Myers AACS, SCO November 11, 2003). For T5, I do not have a number for the tumble density, but for T7, it is $16 \times 10^{-10} \text{ kg m}^{-3}$. But for T5, we have a DC average of the thruster firing rate of $\sim 20\%$, as given on page 21 of Reconstruction of Titan-5 Atmospheric Density Using Spacecraft AACS Flight Data, Final AACS Analyses, Attitude and Articulation Control Subsystem (AACS), Cassini Spacecraft Operations Office (SCO), May 16, 2005. Presumably, the tumble density is defined as that density where the average thruster firing rate is 100%, so on T5 multiplying the AACS mass densities of $(5.7 - 6.8 \times 10^{-10} \text{ kg m}^{-3})$ by 5, we get $(28.5 - 34 \times 10^{-10} \text{ kg m}^{-3})$. But these values are a factor of 2 higher than the T3 and T7 numbers.

The first task is to define the correspondence between the tumble density and maximum thruster firing rate, based on an average over some interval of time. If we use the tumble density criterion and assume atmospheric densities on T7 will be identical to those of TA, a 1025 km flyby with AACS inferred densities of $15 - 21 \times 10^{-10} \text{ kg m}^{-3}$ would imply the spacecraft will encounter densities at TCA almost equal to or in excess of the tumble density, but will have an average thruster firing rate of $\sim 50\%$.

Once the correct criterion is settled, I suggest using the INMS mass density profiles as the most accurate for the density variation with altitude and to use the T5 INMS density at 1027 km to infer the correspondence between INMS density and thruster firing rate. Then assume that on T7 we will encounter densities equal to TA. Determine the flyby altitude based on the correct link of tumble density with thruster firing rate and, of course, with appropriate margin for trajectory delivery errors, that the atmospheric density may be higher than TA, etc.

Appendix 2: Update on the Discrepancy in Mass Density Inferred by AACS and INMS

D.F. Strobel (circa Late 2004)

Update On the Discrepancy in Mass Density Inferred by AACS and INMS

According to Allan Lee, the mass density at TCA on flyby Ta was inferred with the following formula for the torque imparted on the spacecraft, $\vec{T}_{atmosphere}$:

$$\vec{T}_{atmosphere} = C_d \frac{1}{2} \rho V^2 A_{project} (\vec{c}\vec{p} - \vec{c}\vec{m}) \times (-\vec{u}_V) \quad (1)$$

where the drag coefficient $C_d = 2.07$, the velocity $V = 6.06 \text{ km s}^{-1}$, the area $A_{project} = 16.4 \text{ m}^2$, the difference between the center of pressure and center of mass $(\vec{c}\vec{p} - \vec{c}\vec{m}) = 0.985 \text{ m}$, and \vec{u}_V is a unit vector. The maximum inferred torque at TCA from thruster firings was 0.103 N m . Substitution of these values into Eq. (1) gives $\rho = 1.7 \times 10^{-10} \text{ kg m}^{-3}$ at TCA = 1174 km altitude, whereas INMS measured $\rho = 4.7 \times 10^{-11} \text{ kg m}^{-3}$ at the same altitude.

In an attempt to understand the discrepancy in inferred mass density, I looked at the engineering blueprints that the MAG team had at Imperial College, when I attended the London Titan Seminar Series, earlier this week. When looking at the spacecraft along the x-axis, it looks fairly symmetrical with respect to the z-axis, with the exception of the magnetometer boom. I decided to estimate the torque imparted on the spacecraft by assuming that 1) the only asymmetry is the magnetometer boom, 2) the center of mass lies on the z-axis, and 3) the radius of the spacecraft is 2 m. According to the engineering drawings, the boom extends 433 inches (= 11 m) from the z-axis along the -y-axis and has a thickness projected on the z-axis of 27.25×0.4 inches (= 0.28 m). (Here 27.25 inches is offset of the axis of the boom from $z = 0$ and using a ruler, I estimated the thickness at 0.4 times this offset. This is definitely low tech engineering.) The atmospheric torque is thus

$$\vec{T}_{atmosphere} = C_d \frac{1}{2} \rho V^2 \int_2^{11} y \, dy \int_0^{0.28} dz = C_d \frac{1}{2} \rho V^2 \left[\frac{y^2}{2} \right]_2^{11} 0.28 \quad (2)$$

$$\vec{T}_{atmosphere} = C_d \frac{1}{2} \rho V^2 16.4 \quad (3)$$

Comparison of Eqs. (1) and (2) indicate that

$$A_{project}(\vec{c}\vec{p} - \vec{c}\vec{m}) = 16.2 =? \int_2^{11} y \, dy \int_0^{0.28} dz = 16.4 \quad (4)$$

and thus confirms the AACS analysis, if my assumptions are essentially correct.

$$\vec{T}_{atmosphere} = C_d \frac{1}{2} \rho V^2 \int_2^{11} y \, dy \int_0^{0.28} dz = C_d \frac{1}{2} \rho V^2 16.4 \quad (5)$$

According to Allan Lee at TCA the thruster duty cycle was operating at 6.3% of its maximum capability. Hence the maximum mass density that the thrusters can handle is $1/0.063 = 15.87$ times the TCA mass density or

$$\rho_{crit} = \frac{1}{0.063} \times 1.7 \times 10^{-10} = 2.7 \times 10^{-9} \text{ kg m}^{-3} \quad (6)$$

Extrapolate the mass density to lower altitudes using an isothermal atmosphere with gravitational acceleration varying as r^{-2} . The Jeans λ parameter is

$$\lambda(r) = \frac{r}{H(r)} = \frac{m_{av}g(r)r}{kT} = \frac{\text{gravitational potential energy}}{\text{random kinetic energy}} \quad (7)$$

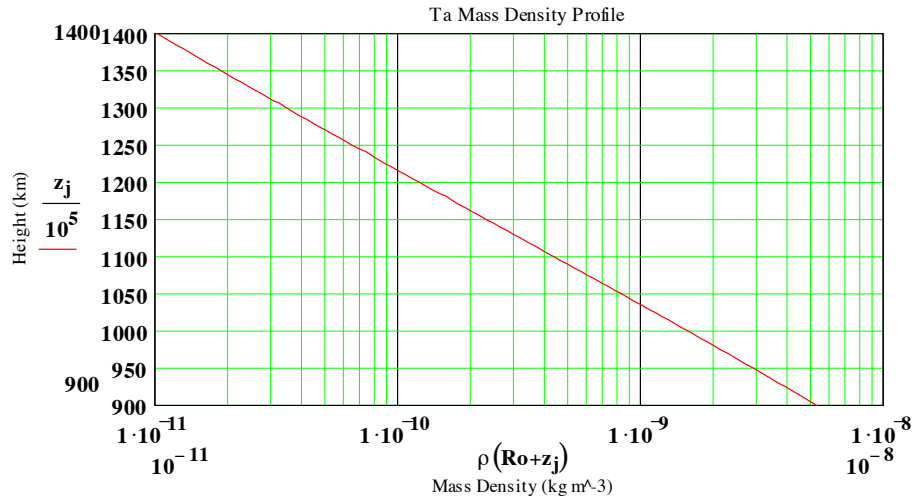
and

$$\frac{\rho(r)}{\rho_{TCA}} = \exp[\lambda(r) - \lambda(r_{TCA})] \quad (8)$$

where r is the radial distance from the center of Titan, $m_{av} = 27.8$ amu times amu in kilograms, $T = 153.6$ K, and $\lambda(r_{TCA}) = 52.06$. Consequently, the critical λ is

$$\lambda(r) = \lambda(r_{TCA}) + \ln\left(\frac{1}{0.063}\right) = 52.06 + 2.765 = 54.83 \quad (9)$$

and the "minimum" flyby altitude is 955 km WITH NO MARGIN. Note that this altitude is independent of the absolute mass density, since it is based on the ratio of actual percentage thruster firings at TCA versus the maximum of 1. The mass density profile in the figure below should be regarded as "correct" for height profile, but uncertain in absolute magnitude.



What are the bounds on the drag coefficients? The Knudsen number on the basis of the INMS mass density is $Kn \sim 240$ at TCA, whereas on the basis

of AACs torques, it is ~ 60 . When $\text{Kn} > 10$, free molecular flow conditions apply. Since the spacecraft torque is due to the magnetometer boom and for hypersonic free molecular flow, $C_d \rightarrow 2$ for diffuse reflection and $\rightarrow 2.67$ for specular reflection based on its cylindrical shape. A conservative upper bound on the drag coefficient can be obtained by assuming that the boom is a flat rectangular plate perpendicular to the spacecraft velocity vector. Then $C_d \rightarrow 2$ for diffuse reflection and $\rightarrow 4$ for specular reflection. While $C_d = 4$ is a rigorous upper bound and would not account for the factor of 4 discrepancy in mass density, a more realistic upper bound is $C_d = 2.67$, as the boom is effectively a cylinder.

If we adopt the upper bound on $C_d = 2.67$, then substitution of this value into Eq. (1) gives $\rho = 1.3 \times 10^{-10} \text{ kg m}^{-3}$ at TCA = 1174 km altitude, and the discrepancy would be reduced to 2.8.

What do we know about the properties of the magnetometer boom and the material wrapped around it? Specifically, what are the thermal accommodation coefficients, α , the normal reflection coefficients, σ_n , and the tangential reflection coefficients, σ_t ? Note that for specular reflection $\alpha = \sigma_n = \sigma_t = 0$, whereas for diffuse reflection $\alpha = \sigma_n = \sigma_t = 1$. Most materials have the latter property, but could we have exceptions for the magnetometer boom components?

Another concern is that while the Knudsen number is in the range of 60-240, we know that a hypersonic spacecraft creates a snowplow effect as it moves through the atmosphere. The number density enhancement in gas adjacent to the spacecraft surface for diffuse reflection is (Bird, Planet. Space, Sci., 36, 921, 1988):

$$\frac{n}{n_\infty} = \frac{1}{2} \{ [1 + \text{erf}(s \cos \theta)] \times [1 + \sqrt{\pi} s \cos \theta \sqrt{\frac{T_\infty}{T_{sc}}} + \sqrt{\frac{T_\infty}{T_{sc}}} \exp(-s^2 \cos^2 \theta)] \} \quad (10)$$

where ∞ denotes free stream quantities, T_{sc} is the spacecraft surface temperature, θ is the angle between velocity vector and normal to surface, and s is the speed ratio = $V_{sc} / \sqrt{\frac{2kT_\infty}{m_i}}$ for a constituent with molecular mass m_i . I estimate this enhancement to be ~ 50 for N_2 . Thus the Knudsen number in the vicinity of the spacecraft drops to 1-5 and one is no longer strictly in the free molecular regime (usual criterion is $\text{Kn} > 10$). Note that this number density enhancement is essentially the dynamic ram density enhancement factor for INMS in free molecular flow

$$\frac{n_{INMS}}{n_\infty} = \sqrt{\frac{T_\infty}{T_{INMS}}} \{ \sqrt{\pi} s \cos \theta \times [1 + \text{erf}(s \cos \theta)] + [\exp(-s^2 \cos^2 \theta)] \} \quad (11)$$

which I also estimate to be ~ 50 . I have used in these estimates $T_{sc} = 75$, $T_{INMS} = 273$, $T_\infty = 150$ K. How well do we know the first two temperatures? INMS assumes complete thermal accommodation to the "wall" temperature. How is this expression modified as one enters the transition regime flow when $\text{Kn} \sim 1$?

Bird (AIAA Journal, 4, 55, 1966) predicted a drag coefficient overshoot over the free molecular value in the range of $Kn \sim 0.5-20$, which has been verified by experiments (e. g. Koppenwallner, Drag and Pressure Distribution of a Circular Cylinder at Hypersonic Mach Numbers in the Range between Continuum Flow and Free Molecular Flow, in Rarefied Gas Dynamics, 6th Symp., Vol. I, Suppl. 5, Academic Press, 739, 1969 - there are probably better references, but the Observatoire de Paris is not noted for its aerodynamics library collection). It would be worthwhile to do a DSMC of the Cassini spacecraft's interaction with Titan's upper atmosphere.

In summary there is no "smoking gun" to remove the factor of 4 discrepancy between AACCS and INMS. Whether one can whittle down this discrepancy by multiplet increments and get within or better than a factor of 2 eventually, where most of us would feel comfortable with error bars $\pm 30\%$, is uncertain. But the Project definitely needs to understand this discrepancy and resolve it, if possible. A good start would be to get NASA Langley involved with DSMC calculations.